Carbon sequestration and storage in Norwegian Arctic coastal wetlands: impacts of climate change

Raymond D. Ward[1,2]

[1] Centre for Aquatic Environments, University of Brighton, Moulsecoomb, Brighton, BN2 4GJ, United Kingdom.

[2] Institute of Agriculture and Environmental Sciences, Estonian University of Life Sciences, Kreutzwaldi 5, EE-51014 Tartu, Estonia

Highlights:

- Arctic coastal wetlands store less carbon than global averages due to thin soils.
- Carbon sequestration rates are similar to those of temperate salt marshes.
- Extension of the growing season has resulted in increased carbon sequestration.

Abstract

Coastal wetlands contain some of the largest stores of pedologic and biotic carbon pools, and climate change is likely to influence the ability of these ecosystems to sequester carbon. Recent studies have attempted to provide data on carbon sequestration in both temperate and tropical coastal wetlands. Alteration of Arctic wetland carbon sequestration rates is also likely where coastal forcing mechanisms interact directly with these coastal systems. At present there are no data available to provide a detailed understanding of present day and historical carbon sequestration rates within Arctic coastal wetlands.

In order to address this knowledge gap, rates of carbon sequestration were assessed within five Arctic coastal wetland sites in Norway. This was undertaken using radiometric dating techniques (^{210}Pb and ^{137}Cs) to establish a geochronology for recent wetland development, and soil carbon stocks were estimated from cores.

Average carbon sequestration rates were varied, both between sites and over time, ranging between 19 and 603 g C m^2 y^{-1}, and these were correlated with increases in the length of the growing season. Stocks ranged between 3.67-13.79 Mg C ha^{-1}, which is very low compared with global average estimations for similar coastal systems, e.g. 250 Mg C ha^{-1} for temperate salt marshes, 280 Mg C ha^{-1} for mangroves, and 140 Mg C ha^{-1} for seagrasses. This is most likely due to isostatic uplift and sediment accretion historically outpacing sea level rise, which results in wetland progradation and thus a continuous formation of new marsh with thin organic soil horizons. However, with increasing rates of sea level rise it is uncertain whether this trend is set to continue or be reversed.

Keywords:

Salt marshes, climate mitigation, blue carbon, Norway, sediment accretion, increased productivity

1 Introduction

There is a general consensus that over the last century global climate has undergone change including increases in temperature and sea level rise (Rahmstorf 2010), largely as a result of the 40% increase in atmospheric carbon since 1750 (IPCC 2013). There are five major pools of global carbon: oceanic, geologic, pedologic (soil), atmospheric and biotic (Figure 1). Each of these carbon pools is

47 interconnected and the oceanic, pedologic, and biotic pools can be considered as
48 important buffers to climate change, with the oceanic pool being the most stable
49 (Powlson et al. 2011).

50 Chmura et al. (2003) suggested that vegetated coastal ecosystems (salt marshes,
51 mangroves and seagrasses) contain the largest stores of pedologic and biotic
52 carbon (termed as blue carbon). This provides an important ecosystem service by
53 removing carbon from the atmosphere, although the majority of studies assessing
54 global carbon budgets have focussed on forests and grasslands.

55 A range of studies state that climate change is likely to influence the ability of
56 wetlands to sequester carbon (Delaune and White 2011; Bianchi et al. 2013;
57 Doughty et al. 2016; Osland et al. 2016; Ward et al. 2016; Mafi-Gholami et al. 2018;
58 Saintilan et al. 2019), particularly in high latitudes due to changes in the length of the
59 growing season (Chmura et al. 2003).

60 The effects of climate change on coastal wetlands are more complex than on interior
61 wetlands due to the greater amount of influencing factors such as increased
62 storminess, alterations to precipitation regimes, sea level rise, and in very high
63 latitudes, changes in the concentration and duration of land-fast sea ice (Ward et al.
64 2014; Ward et al. 2016a; Ward et al. 2016b; Mafi-Gholami et al. 2018; Lima et al.
65 2020). These factors are often combined with other global change impacts including
66 population growth, land use-land cover change, environmental pollution, which can
67 impact sedimentary, geochemical and geomorphology of coastal ecosystems (Ward
68 et al. 2014; Celis Hernandez 2020; Bardos et al. 2020; Veettil et al. 2020).

69 Recent studies have attempted to provide data on carbon sequestration in both
70 temperate and tropical coastal wetlands (Li et al. 2010; Kirwan & Mudd 2012;

Pendleton et al. 2012; Smoak et al. 2013; Duarte et al. 2013; Lovelock and Duarte 2019). However, there has been no attempt to assess carbon sequestration or stocks within Arctic coastal wetlands, despite the extent of the Arctic Ocean coastline (45389 km) (Symon et al. 2005), equivalent to the Atlantic coastline of the Americas. Furthermore, climate change has already disproportionately impacted the Arctic region (IPCC 2013) with changes including significant reductions of summer and land-fast sea ice cover (Ding et al. 2017). Symon et al. (2005) suggest that this is likely to result in an alteration in coastal processes and more dynamic coastal environments.

Temperature increases and resultant extensions to the growing season are also likely to increase net primary productivity (Symon et al. 2005), with resultant changes in rates of carbon sequestration, particularly in ecosystems at the interface of marine and terrestrial systems. Significant alteration to Arctic wetland carbon sequestration is also likely where coastal forcing mechanisms interact directly with these coastal systems. At present, there are no data available to provide a detailed understanding of present day and historical carbon sequestration rates within Arctic coastal wetlands. Such data are essential for making any assessment of carbon storage within these ecosystems and of future trends in response to the continued warming of the Arctic region.

In order to address this knowledge gap, this study assessed rates of carbon sequestration within Arctic coastal wetlands and identified drivers of changes in rates over the last 150 years using radiometric dating techniques (^{210}Pb and ^{137}Cs) to establish a geochronology for recent wetland development.

2. Study area

The study sites are located along the Arctic coast of Norway between Tromsø (69.6492° N, 18.9553° E) and Stabbursnes (70.1613° N, 24.9537° E) (Figure 1, Table 1). In the last ten years average annual precipitation was 551 mm, predominantly falling between July and January (Table 1). Over the same period, average summer temperatures are 10.1°C with a short growing season of ~120 days (where temperatures are > 5°C) and average winter temperatures are -3.5°C (Table 1). Plant productivity is quite high within these coastal ecosystems (Dijkema 1990), and Arctic coastal wetlands provide an important habitat for hundreds of thousands migratory geese, ducks and charadriiformes (Henningsson and Alerstam 2005). The plant communities are substantially influenced by cattle, reindeer and goose grazing and typically consist of *Puccinellia phryganodes*, *Puccinellia retroflexa borealis*, *Cochlearia officinalis*, *Carex subspathacea*, *Festuca rubra*, *Carex glareosa*, *Carex mackenziei*, and *Juncus gerardii* (Martini et al. 2019).

The Arctic mainland of Norway has an uplifting coastline with a rate of ~1mm yr^{-1} (Eronen et al. 2001), similar to rates occurring in Scotland and south Estonia where it has been suggested that recent sea level rise is now outpacing combined coastal wetland sediment accretion and uplift (Teasdale et al. 2011; Ward et al. 2014). Arctic coastal wetlands in Norway are typically located at the head of deep fjords with small estuaries which drain from the surrounding mountain catchments and glaciers. The size of the wetlands is dependent on available sediment deposition and inheritance, which provides a shallow platform to the typically deep and steep coastline within the fjords (Martini et al. 2019).

The bedrock surrounding the fjords consists of Precambrian-Silurian crystalline rocks (Levell 1980) with Mesozoic sedimentary rocks within the coastal areas (Roberts et

al. 1997) overlain by between 50-200m of Quaternary sediments dependent on location within the fjord channels. Coastal sediments are of periglacial/ glacial origin e.g. glacial moraines, glacio-fluvial deposits, fluvial deposits, sea-fjord deposits and thick marine deposits (NGU 2017). Fjords are typically between 150-280 m deep although within the Porsanger and Alta depth is substantially less (~15m at the head of the fjords), which results in extensive intertidal mudflat and salt marsh coverage. The banks of the fjords form the boundary between the sedimentary and crystalline rocks (NGU 2017). The Norwegian Current and the Coastal Current are the dominant marine currents in the region, bringing warm water flowing to the northeast. The Coastal Current has the strongest influence on the hydrodynamics of the fjords in Finnmark (Wassmann et al. 1996). Sea surface temperatures within the fjords fluctuate between 5 and 11°C throughout the year (Eilertsen and Skarðhamar 2006). The five study sites were selected to take into account the variability in Norwegian Arctic coastal wetlands consisting of the two largest coastal wetlands in the region (Alta within Altafjord and Stabbursnes within Porsangerfjord) and smaller fjordhead coastal wetlands, similar to those of Scotland, that are typical of the region (Birtvarre, Storfjord and Storslett) (Figure 2). The Alta coastal wetland is adjacent to Altaelva, one of the largest rivers in the region, providing a substantial supply of sediments to the site (Figure 2a). Stabbursnes is located at the mouth of the small, steep mountain fed Stabburselva (Figure 2b). Birtvarre is located at the head of Kå fjord, and the coastal wetland is located at the mouth of Kåfjordelva (Figure 2c). Storfjord is located at the head of Lyngen fjord and the coastal wetland is at the mouth of Signaldaelva (Figure 2d). Storfjord is located at the head of Reisa fjord and the coastal wetland is at the mouth of Reisaelva, this site is the least sheltered from the open ocean (Figure 2e).

3. Material and methods

3.1 Field data collection

Two soil cores (75 mm diameter, depth to refusal) were collected using a stainless-steel Russian corer, within each of the five coastal wetlands (Stabbursnes, Storslett, Birtvarre, Alta, and Storfjord, a total of ten cores) following a walkover survey to visually determine the heterogeneity (which was limited) of the soil profile within each site. Refusal, was at all times a thick (>1m depth), minerogenic glacio-fluvial cobble/ boulder layer with a very low organic matter content. Cores were selected from the low and high marsh ecological zones within each site, with the low marsh typically inundated at each high tide and the high marsh inundated only during spring high tides. The high marsh typically consisted of *Carex subspathacea* mixed with *Puccinellia phryganodes* (Storfjord, Alta, Birtvarre), *Carex subspathacea* mixed with *Festuca rubra* (Storslett), and *Carex subspathacea* mixed with *Juncus gerardii* (Stabbursnes). The low marsh was dominated by *Juncus gerardii*.

Each core was inserted into the soil ensuring minimal compaction (<5% as per Ward et al. 2014). These samples were sealed in the field, removed intact and frozen within 4 hours of collection for transport to the laboratory for analysis.

3.2 Granulometry and organic matter analysis

Cores were extracted in the laboratory allowing the outer section of the core to defrost enabling extraction from core barrels with no compaction, which was tested by measuring the core both before and immediately after extraction. Cores were then meticulously cleaned and each core was sliced into 0.5 cm depth increment sub-

samples and dried at 40°C until constant weight (to ensure minimal loss of lead isotopes). Total organic matter was estimated using the loss on ignition (LOI) method combusting samples at 450°C for 12 hrs (Bisutti et al. 2004; Lima et al. 2020). The LOI method can have problems with losses of structural water in clays (at temperatures >500°C) and $CaCO_3$ in carbonate soils (at temperatures of 800°C or higher) or incomplete combustion of organic components (typically <400°C). However, this is unlikely to have influenced results for $\%C_{org}$ at these sites due to the very low clay and carbonate content and the temperature of combustion.

Soil organic carbon was estimated from soil organic matter using the equation specifically recommended for blue carbon accounting (Howard et al. 2014):

$$\%C_{org} = 0.47 \times \%LOI + 0.0008 \times (\%LOI)^2$$

Soil organic carbon values were used to calculate carbon density using the equation:

$$\text{Soil carbon density} = \text{dry bulk density} \times (\%C_{org}/100)$$

Dry bulk density was estimated using the equation from Dadey et al. (1992):

$$\text{Dry bulk density} = (1-\phi)P_s$$

Where ϕ = porosity, and P_s = grain specific gravity (in this case 2.5 g/cm^3, Dadey et al. 1992).

Sediment particle size analysis was conducted on samples with organics removed in a Malvern Mastersizer 2000 (Laser PSA). 10ml of sodium hexametaphosphate was added to each sample and this was mixed in a vortex mixer for 5 minutes. Following this samples underwent 30 seconds of ultra-sonication prior to particle size analysis. Texture was categorised using the Wentworth (1922) classification derived from three analytical runs to provide an average (standard error <1%).

3.3. ^{210}Pb and ^{137}Cs dating carbon sequestration rates

In order to estimate rates of carbon sequestration, a core profile geochronology was established. Over short time periods (decades to 150 years), ^{210}Pb dating is a well-established methodology that uses the half-life of this radionuclide (22.6 years) to date specific horizons within the soil profile (Wise 1980; Cundy and Croudace 1996; Plater and Appleby 2004; Ward et al. 2014). The geochronology was calculated using the Constant Rate of Supply (CRS) model (Appleby and Oldfield 1992). The CRS model provides a detailed geochronology using inventories to calculate date of deposition for each depth within the soil profile which can be used to identify the variation in carbon sequestration rates over time. For dating purposes, the supported component was assessed via direct measurement of the daughter radionuclide ^{214}Pb, in conjunction with the estimation of constant ^{210}Pb activity at depth. In this study ^{214}Pb closely approximated ^{210}Pb at the lowest depths of the core, thus indicating that the measurement of ^{214}Pb is a robust proxy for supported ^{210}Pb (Brown et al. 2019).

^{137}Cs in soils is predominantly derived from global inputs from the detonation of nuclear weapons prior to the Partial Test Ban Treaty in 1963 (Ritchie and McHenry 1990) and in Europe from the Chernobyl nuclear reactor accident in 1986 (Anspaugh et al. 1988), which strongly impacted on northern and eastern European nations including Norway.

^{210}Pb and ^{137}Cs down core activity profiles were obtained at a depth resolution of 0.5 cm and determined using a Canberra ultra-low background high purity germanium well-type gamma spectrometer. Background emission subtractions are undertaken

on a fortnightly basis and energy and efficiency calibrations were made with a mixed gamma-emitting radionuclide standard, QCYK8163. The limits of detection vary with radionuclide, sample mass and count times, but these were 8 Bq kg^{-1} for ^{210}Pb, and 1 Bq kg^{-1} for 137Cs, for a 260,000 second count time, where required extended count times were conducted.

Carbon sequestration rates (C_{seq}, g C m^2 $year^{-1}$) were calculated using the rate of sediment accretion (cm yr^{-1}) derived from the ^{210}Pb CRS geochronology data multiplied by the density of soil C (g cm^{-3}) (Greiner et al. 2013):

Cseq = C density x sediment accretion rates.

3.4 Comparing carbon sequestration with environmental and meteorological variables

Glacial Isostatic Adjustment (GIA) calibrated sea level data collated from the Norwegian Mapping and Cadastre Authority archives (NGU 2017) were obtained for the three nearest tide gauge stations to the study sites, which were Tromsø, Honningsvåg, and Hammerfest, with the closest allocated to the corresponding study site. Additionally, climate data were obtained from the Norwegian Meteorological Institute archives (MET Norway 2019), including mean annual precipitation and length of the growing season (calculated as number of days per year where temperatures exceeded 5°C, Ratas and Nilson 1997). These data were available at a daily resolution from late 1800's (Alta), early 1950's (Stabbursnes, Storslett) and the early to mid-1960's for Birtvarre and Storfjord. Sea level, precipitation and growing season data were averaged for each period (inter-dated horizons up to a maximum of a decade) relating to the geochronologies derived from the ^{210}Pb dating

for the soil profiles. These data, combined with d50 and sorting coefficients (Trask 1932) for corresponding soil horizons, were compared with the dated carbon sequestration rate results using a Pearson's test for correlation (Lima et al. 2020) to evaluate the relationships between these environmental factors and carbon sequestration.

4. Results and interpretation

4.1 Sediment characterisation

Within both the low and high marsh cores from Alta, the soil predominantly consisted of sand, as was the case for the cores from the low marsh at Storfjord (Figure 3a, b). The high marsh cores from Stabbursnes and Birtvarre were also predominantly sand (Figure 3d, f), with substantial gravel fractions and no clay. The most recently deposited sediments were predominantly silt in the low marsh cores from Stabbursnes and Birtvarre (from the 1990s to present, Figure 3c, e), a change from predominantly sand fractions in older soils. The same trend can be seen in the low and high marsh cores from Storfjord (1950s and 1940s respectively, Figure 3g, h). Clay fractions were highest in the low marsh cores from Stabbursnes and Birtvarre and in the upper marsh cores from Storfjord and Storslett (between 1 and 10%, Figure 3c, e, h, and j respectively).

Organic matter varied substantially both between sites and down the cores. At Alta organic matter did not exceed 5% (Figure 4a,b) and was lowest at the very bottom of the lower shore core where it reached the low organic cobble bed. The Stabbursnes and Birtvarre cores showed the highest organic matter, which was evident in the walkover study. Values ranged from 12 - 54% in the upper layers (Figure 4c,d,e,f),

although variation was much lower in the dateable stratigraphy, particularly for Birtvarre. At Storfjord low marsh, there was substantial variation in the upper dateable stratigraphy (Figure 4g), this was less pronounce in the upper marsh core (Figure 4h). At Storslett low marsh the organic matter content was quite low (~4%) and varied within the upper dateable stratigraphy (Figure 4i). In the Storslett high marsh core, organic matter was much higher, up to 31% in the upper stratigraphy (Figure 4j), this decreased to 3 - 4%, with an exceptional band of highly organic material between 20 - 24cm deep.

4.2. ^{210}Pb and ^{137}Cs dating

^{137}Cs was found in all cores within the five study sites and there were two peaks identified within each core (Figure 5). These were related to a deeper peak in ^{137}Cs activity derived from global atmospheric deposition as a result of above ground nuclear weapons testing reaching a peak in 1963 and a shallower profile peak related to the 1986 Chernobyl nuclear disaster. There is some evidence for post depositional migration of ^{137}Cs in all cores, highlighted by broadening of peaks, particularly in the Storfjord cores (Figure 5g, h). ^{137}Cs was also evident at depths that predate the occurrence of this artificial radionuclide as well as in surface sediments, in spite of there being no recent records of addition (Table 2). Within the Alta low marsh core (Figure 5a) there are additional peaks in ^{137}Cs activity, which is likely to be linked to reworking of older sediments and relocation in shallower horizons within the soil profile. There was a broad agreement between dating between ^{210}Pb and ^{137}Cs, although not within the Alta high marsh and Storslett low marsh cores (Table 2). There was also weak agreement between the ^{210}Pb and ^{137}Cs dates for the

Storfjord low and high marsh and Storslett high marsh for 1963 (Table 2), most likely due to post depositional remobilisation of 137Cs.

Average carbon sequestration rates derived from ^{137}Cs were lowest at Alta, the site with highest fluvial inputs, in the low and high marsh over both recorded time periods, 1963 and 1986 (Table 3). The highest recorded rates of carbon sequestration were recorded for Storfjord low marsh 1337 gC m^2 $year^{-1}$ over the period 1963 to present and 1569 gC m^2 $year^{-1}$ over the period 1986 to present.

The ^{210}Pb downcore profiles show evidence of exponential decay, to background, with initial concentrations of 100-350 Bq kg^{-1} (Figure 6), with the exception of the Alta cores where initial concentrations were substantially lower (18-48 Bq kg^{-1} Figure 6a, b for low and high marsh respectively). The low concentrations at Alta are most likely the result of erosion of surface sediments. Background concentrations of ^{210}Pb were 6-36 Bq kg^{-1}, and these were estimated using ^{214}Pb which is in secular equilibrium.

Soil horizons dated using the CRS method provided the oldest dateable sediments between 1870 and 1930, which is within the accepted limits of dating for this method (100-150 years) (Figure 7). The maximum depth that was able to be dated was within the Storfjord low marsh core (10.75 cm) (Figure 7g) representing a date of 1909 and the shallowest was in the Storslett high marsh core at 4.75 cm representing a date of 1870 (Figure 7j). It should be noted that the ^{210}Pb and ^{137}Cs dating may be compromised in the Alta low marsh core as a result of erosion of surface sediments, considering the CRS model assumptions.

4.3 Carbon stocks and sequestration rates

312 Estimated average carbon sequestration rates were lowest from the low and high
313 marsh plant communities at the Alta site (19 and 22 gC m^2 $year^{-1}$, Table 4). Low
314 values were also recorded in the low marsh at the Birtvarre site. Trends in carbon
315 sequestration rates between sites were similar to those recorded using the ^{137}Cs
316 dating method. Values were also similar for all sites with the notable exception of the
317 high marsh for Birtvarre and the low marsh for Storfjord, where values were
318 substantially lower using the ^{210}Pb derived results (973-1277 gC m^2 $year^{-1}$ from ^{137}Cs
319 compared with 603 gC m^2 $year^{-1}$ using ^{210}Pb results for Birtvarre high marsh, and
320 1337-1569 gC m^2 $year^{-1}$ from ^{137}Cs dating compared with 390 gC m^2 $year^{-1}$ using
321 ^{210}Pb results for Storfjord low marsh).

322 The highest carbon sequestration rates were recorded for Storslett low marsh within
323 the most recently formed soils (2117 gC m^2 $year^{-1}$, since 2010, Figure 8i), and the
324 lowest peak sequestration values were recorded in the low and high marsh at Alta
325 (81 and 188 gC m^2 $year^{-1}$) recorded in the mid-1990s and since 2010 respectively
326 (Figure 8a, b). Peaks in carbon sequestration were noted in the most recently formed
327 soils in the low marsh at Stabbursnes (Figure 8c), the high marsh at Alta (Figure 8b)
328 and both the low and high marsh at Storslett (Figure 8i, j).

329 In the walkover study, there was not found to be a substantial variation in the particle
330 size nor organic matter throughout the sites. Carbon stocks were found to range
331 between 3.67 - 13.79 MgC ha^{-1} derived from the cores collected. The upper marsh at
332 Storslett had the highest values recorded, and the upper marsh at Alta had the
333 lowest values (Table 5).

334

335 *4.4. Comparison between environmental and meteorological variables and carbon*
336 *sequestration rates over time*

Results from the tests for correlation between GIA corrected sea level rise, length of the growing season, average annual precipitation, D50, and sorting coefficient showed that only length of the growing season was significantly correlated with carbon sequestration rates ($r = 0.815$, $p < 0.001$, Table 6), and the extension of the growing season results in increased carbon sequestration. Average annual precipitation was significantly correlated with D50 ($r = 0.651$, $p = 0.02$), although not with carbon sequestration rates (Table 6).

5. Discussion

5.1 Radiometric dating

^{137}Cs was found at all sites and exhibited a typical profile for the region (Ward et al. 2014; Ward 2020), with two primary peaks. The deeper peak related to the pre-1963 above ground nuclear weapons testing and a shallower peak related to the 1986 Chernobyl nuclear incident. There appears to have been some post depositional remobilisation of the ^{137}Cs due to its location at the surface, which post-dates recorded inputs, and deep in the sediment profile prior to the occurrence of this artificial radionuclide. ^{137}Cs activity within the soil profile is within the range of published values for the region of 4-80 Bq kg^{-1} (Callaway et al. 1996; Cundy and Croudace 1996; Andersen et al. 2001; Povinec et al. 2003; Teasdale et al. 2011; Ward et al. 2014). There is also some evidence of broadening of the ^{137}Cs activity peaks in the sediment profile, particularly notable within the Storfjord low and high marsh cores (Figure 5g, h). Previous studies have shown that in cores with high proportions of soil organic matter post depositional mobility of ^{137}Cs is enhanced (Ritchie and McHenry 1990; Rosen et al. 2009; Ward et al. 2014), as is likely to be

361 the case in these Arctic coastal wetland soils. Other studies have suggested that this
362 is likely to be exacerbated in coarse grained soils where there are small fractions of
363 fine sediments, particularly clay (Borretzen and Salbu 2002; Teasdale et al. 2011).
364 Borretzen and Salbu (2002) demonstrated that following deposition, there is rapid
365 adsorption of ^{137}Cs to clay fractions. The low clay content of the soils in the studied
366 Arctic coastal wetlands is likely, at least in part, to be the cause for the broadening of
367 the ^{137}Cs peaks. There is also likely to be horizontal percolation of sea water through
368 these coarse-grained soils during tidal or storm induced inundation, which increases
369 pore water pressure and has been suggested as a mechanism for post depositional
370 relocation of ^{137}Cs to surface sediments (Harvey et al. 1995; Thompson et al. 2001;
371 Teasdale et al. 2011). However, similar results obtained using both the ^{210}Pb and
372 ^{137}Cs dating methods suggest that these are reliable and provide a robust validation
373 dataset (Ward 2020).

374 All cores showed a near exponential decay of ^{210}Pb from the surface to background
375 levels estimated using ^{214}Pb, indicating a constant supply of atmospherically derived
376 ^{210}Pb, which is implicit in the assumptions for the CRS method (Appleby and Oldfield
377 1992). The cores from both the Alta low and high marsh exhibit much lower ^{210}Pb
378 activity than the other sites, 18 and 47 Bq kg^{-1}, which suggests that surface erosion
379 is likely to have taken place, and there was visual evidence from the field that there
380 had been erosion and recolonization of the plant community, particularly evident in
381 the sparse vegetation of the low marsh compared to other sites. Similar ^{210}Pb
382 profiles have been found in Loch Head salt marshes in Scotland (Teasdale et al.
383 2011) and Boreal Baltic coastal wetlands (Ward et al. 2014), in both cases attributed
384 to removal of surface sediments curtailing the ^{210}Pb exponential decrease in activity
385 profile.

386

387 *5.2 Carbon sequestration rates and stocks in Arctic coastal wetlands*

388 Mean carbon stocks across all 5 sites are 6.29 ± 3.35 MgC ha^{-1} taken from cores
389 driven to refusal, which in this case was a thick (>1m depth), minerogenic glacio-
390 fluvial cobble/ boulder layer with very low organic matter content (<0.001%) rather
391 than bedrock. This can be compared with global average values compiled by Duarte
392 et al. (2013), of 162 MgC ha^{-1} for salt marshes, 255 MgC ha^{-1} for mangroves and 140
393 MgC ha^{-1} for seagrasses, which puts Arctic coastal wetlands at the very low end of
394 the carbon stock values. This is most likely in part due to the very thin layer of
395 organic marsh soil (from 9 cm in Birtvarre high marsh to 33 cm in Storslett high
396 marsh), compared with coastal wetlands such as temperate and tropical salt
397 marshes, mangroves and seagrasses, which typically have organic soils >1m
398 (Howard et al. 2014). Furthermore, the historical progradation of these marshes
399 (Martini et al. 2019) suggests that these are relatively young marshes, most likely
400 formed in the last 200 - 300 years, based on the elevation, thickness of the marsh
401 soils, and historical rates of accretion. Ward et al. (2014) found similar results from
402 uplifting coastal wetlands in north Estonia, although unlike the Estonian example, the
403 Arctic coastal wetlands in this study are unlikely to continue progradation due to high
404 rates of sea level rise and low rates of sediment accretion, even accounting for GIA
405 (Ward 2020). There was some geomorphic evidence in Birtvarre, Storfjord and
406 Storslett, of recent erosion of the fore marsh, this further suggests that progradation
407 has at least partially ceased.

408 The highest carbon stocks were recorded for the Storfjord low (10.53 MgC ha^{-1}) and
409 Storslett high marsh (13.79 MgC ha^{-1}) sites (Table 5), and the lowest carbon stocks
410 were recorded for Alta low and high marsh (3.79 and 3.67 MgC ha^{-1}, Table 5). It is

likely the low values for the Alta site are due to a substantial minerogenic input from fluvial sources due to its location at the mouth of the 3rd largest river in the region, the Altaelva river. It was also noted that there was a lower surface activity of ^{210}Pb in the low and high marsh at Alta than all other sites (Figure 6), suggesting that there has been erosion of the surface sediments. Similar results, where erosion influences carbon stock values, have been found for other vegetated coastal environments including salt marshes in Scotland (Teasdale et al. 2011), Boreal Baltic coastal wetlands (Ward et al. 2014), and temperate seagrasses (Lima et al. 2020).

The high values for carbon stocks recorded for the Storfjord low marsh and the Storslett high marsh were a result of a combination of deeper organic soil profile and high carbon density. Both of these sites are likely to have the oldest wetlands, considering the rates of accretion and the depth of the organic soil horizon compared to the other sites (Figures 4 and 8).

Average rates of carbon sequestration over the whole dated time period varied from 19 to 603 gC m^2 $year^{-1}$, comparable to global average rates of sequestration for salt marshes at 218 gC m^2 $year^{-1}$ (Duarte et al. 2013). This further supports the suggestion that the reason Arctic coastal wetlands have low carbon stocks is due to their relatively young age as a result of GIA, through the continuous formation of new marsh from lower intertidal and sub tidal ecosystems, as has been found in other uplifting coastal wetlands (Teasdale et al. 2011; Ward et al. 2014).

The results of the analysis of environmental and meteorological factors influencing carbon sequestration, showed that the length of the growing season was found to have a significant influence, although there were no other significant correlations. Temperatures have been widely noted as rising higher, and more rapidly, in the Arctic than in any other global region (IPCC 2013). These increases in temperature

436 have been linked to extensions in the growing season, particularly in Eurasia (Park
437 et al. 2016). It has been noted that in temperature limited systems, such as the
438 Arctic, recent warming driven by climate change has resulted in greater plant
439 productivity (Symon et al. 2005; Walker et al. 2012; Forkel et al. 2016; Ju and Masek
440 2016; Park et al. 2016; Yu et al. 2017). This appears to be leading to increases in
441 rates of carbon sequestration in Arctic coastal wetlands, although it is unclear if
442 changes in carbon inputs are as a result of *in-situ* production or supplied by
443 associated terrestrial or marine systems. In a study of in-situ carbon sequestration
444 based on micrometeorological flux tower data, rates of removal of atmospheric CO_2
445 were high in a range of wetlands in the north American and European Arctic, with the
446 highest rates being found in coastal wetlands (Coffer and Hestir 2019). These
447 researchers also found that the coastal wetland sites had increasing rates of *in-situ*
448 carbon sequestration, whereas the inland wetland sites were exporting carbon.
449 Similar results have been found for freshwater wetlands and heath in the Alaskan
450 Arctic, where these ecosystems were also found to be recent exporters of carbon as
451 a result of recent warming trends (Euskirchen et al. 2017).

452 Historical progradation of Arctic coastal wetlands has been suggested to be
453 reversing as a result of decreases in rates of GIA, increases in sea level rise and low
454 sediment accretion rates (Ward 2020). This is likely to lead to an increase in the
455 hydroperiod resulting in an increase in accommodation space, rather than the
456 historical process whereby, new soils have been continually formed and older marsh
457 soils eventually become terrestrial. In this scenario, this is likely to lead to an aging of
458 marsh soils, and potentially as a result greater carbon stocks, particularly where
459 there is greater organic matter input as a result of general warming trends as
460 suggested by the results of this study.

6 Conclusions

The results of this study provide the first assessment of carbon stocks and sequestration rates for Arctic coastal wetlands and suggest that these ecosystems are responding to warming by increasing carbon stocks and rates of sequestration as a result of increased plant productivity; however, it is uncertain if this is *in situ* or from proximate terrestrial and/ or marine systems.

Rates of carbon sequestration are similar to those reported for salt marshes from other global regions. While carbon stocks in the area appear to be increasing, they are still low compared with other climatic regions. This is mostly as a result of the young age of Arctic coastal wetlands due to historical GIA processes and resultant historical formation of new marsh from low intertidal sand/mudflats, and subsequent transformation of old marsh to other fully terrestrial plant communities. This historical progradation of Arctic coastal wetlands is likely to have been reversed, meaning that there is also likely to be a thickening of organic rich soils. Thus, it is clear that Arctic coastal wetlands provide an important ecosystem service through storing and sequestering carbon in their soils and that this ecosystem service is expected to be increased rather than diminished, unlike in other Arctic ecosystems.

Acknowledgements

This research was supported by SETRIF funding from the University of Brighton.

Figure and Table captions:

Figure 1: Five study sites within Norway: Storfjord, Birtvarre, Storslett, Alta and Stabbursnes.

Figure 2: Location of the study sites, showing the proximity to fluvial sources, constaints to migration (e.g.roads and other infrastructure) as well as the area of the site.

Figure 3: Stratigraphy of the core sequences showing percentage of clay, silt, sand and gravel using the Wentworth (1922) classification for all sites (a: Alta low marsh; b: Alta high marsh; c: Stabbursnes low marsh; d: Stabbursnes high marsh; e: Birtvarre low marsh; f: Birtvarre high marsh; g: Storfjord low marsh; h: Storfjord high marsh; i: Storslett low marsh; and j: Storslett high marsh).

Figure 4: Stratigraphy of the organic matter derived from loss on ignition (LOI) for all sites (a: Alta low marsh; b: Alta high marsh; c: Stabbursnes low marsh; d: Stabbursnes high marsh; e: Birtvarre low marsh; f: Birtvarre high marsh; g: Storfjord low marsh; h: Storfjord high marsh; i: Storslett low marsh; and j: Storslett high marsh).

Figure 5: ^{137}Cs activity profiles for all cores at all sites (a: Alta low marsh; b: Alta high marsh; c: Stabbursnes low marsh; d: Stabbursnes high marsh; e: Birtvarre low marsh; f: Birtvarre high marsh; g: Storfjord low marsh; h: Storfjord high marsh; i: Storslett low marsh; and j: Storslett high marsh).

Figure 6: ^{210}Pb activity profiles (circles) for all cores with ^{214}Pb activity shown (triangles) as a proxy for ^{226}Ra and $^{210}Pb_{supported}$ (a: Alta low marsh; b: Alta high marsh; c: Stabbursnes low marsh; d: Stabbursnes high marsh; e: Birtvarre low marsh; f: Birtvarre high marsh; g: Storfjord low marsh; h: Storfjord high marsh; i: Storslett low marsh; and j: Storslett high marsh).

Figure 7: $^{210}Pb_{excess}$ CRS model age/depth profiles for all cores (a: Alta low marsh; b: Alta high marsh; c: Stabbursnes low marsh; d: Stabbursnes high marsh; e: Birtvarre low marsh; f: Birtvarre high marsh; g: Storfjord low marsh; h: Storfjord high marsh; i: Storslett low marsh; and j: Storslett high marsh).

Figure 8: Carbon sequestration rates over time estimated using the 210Pb CRS dating method for all cores at all sites (a: Alta low marsh; b: Alta high marsh; c: Stabbursnes low marsh; d: Stabbursnes high marsh; e: Birtvarre low marsh; f: Birtvarre high marsh; g: Storfjord low marsh; h: Storfjord high marsh; i: Storslett low marsh; and j: Storslett high marsh).

Table 1: Coordinates for all study sites together with length of growing season, average annual temperatures, and average annual precipitation.

Table 2: Comparison between ^{210}Pb and ^{137}Cs dating for the 1963 and 1986 inputs for all cores. BMD = below ^{210}Pb measured dating. EAD = equivalent age depth compared to 1963 dates.

Table 3: Average sequestration rates derived from ^{137}Cs dating.

534

535 Table 4: Average sequestration rates derived from CRS ^{210}Pb dating.

536

537 Table 5: Carbon stocks as calculated from the upper and low marsh for each site.

538

539 Table 6: Matrix results from the Pearson's correlation tests comparing d50, sorting
540 coefficient, rates of sea level rise (GIA corrected), length of the growing season and
541 mean annual precipitation. Results show Pearson's r, and p value (n = 140, * < 0.05,
542 ** < 0.01, and *** <0.001).

543

544 **References**

545 Andersen, T., Mikkelsen, O., Møller, A. and Pejrup, M. (2000). Deposition and mixing
546 depths on some European intertidal mudflats based on 210Pb and 137Cs activities.
547 Continental Shelf Research 20: 1569–1591.

548 Anspaugh, L.R., Catlin, R.J. and Goldman,M. (1988). The global impact of the
549 Chernobyl reactor accident. Science 242: 1513–151

550 Appleby, P. (2001). Chronostratigraphic techniques in recent sediments. Tracking
551 Environmental Change Using Lake Sediments. Kluwer Academic Publishers,
552 Netherlands, pp. 171–203.

553 Appleby, P. and Oldfield, F. (1992). Application of lead-210 to sedimentation studies.
554 In: Harmon, S. (Ed.), Uranium Series Disequilibrium: Application to Earth, Marine
555 and Environmental Science. Oxford Scientific Publications, UK, pp. 731–783.

556 Bardos, P., Spencer, K., Ward, R.D., Maco, B. and Cundy, A.B. (in press). Integrated
557 and sustainable management of post-industrial coasts. Frontiers in Environmental
558 Science: Toxicology, Pollution and the Environment.

559 Bianchi, T., Mead A., Zhao, J., Li, S., Comeaux, R., Feagin, R. and Kulawardhana,
560 W. (2013). Historical reconstruction of mangrove expansion in the Gulf of Mexico:
561 Linking climate change with carbon sequestration in coastal wetlands. Estuarine,
562 Coastal and Shelf Science 119: 7-16.
563 Bisutti, I., Hilke,I. and Raessler, M. (2004). Determination of total organic carbon –
564 an overview of current methods. TrAC Trends in Analytical Chemistry, 23: 10–11.
565 Borretzen, P. and Salbu, B. (2002). Fixation of Cs to marine sediments estimated by
566 a stochastic modelling approach. Journal of Environmental Radioactivity, 61: 1–20.
567 Brown, D.R., Johnston, S.G., Santos, I.R., Holloway, C.J., & Sanders, C.J. (2019).
568 Significant organic carbon accumulation in two coastal acid sulfate soil wetlands.
569 Geophysical Research Letters, 46: 3245-3251.
570 Callaway, J., DeLaune, R. and Patrick Jr., W.H. (1997). Sediment Accretion Rates
571 from Four Coastal Wetlands along the Gulf of Mexico. Journal of Coastal Research,
572 13(1): 181-191.
573 Celis-Hernandez, O., Giron-Garcia, P.M. Ontiveros-Cuadras, J., Canales-Delgadillo,
574 J., Pérez-Ceballos, R., Ward, R.D., Acevedo-Gonzales, O. and Merino-Ibarra, M. (in
575 press). Environmental risk of heavy metals in mangrove ecosystems: An assessment
576 of natural vs oil and urban inputs. Science of the Total Environment, 730: 138643.
577 Chmura, G., Anisfield, S., Cahoon, D. and Lynch, J. (2003). Global carbon
578 sequestration in tidal, saline wetland soils. Global Biogeochemical Cycles 17(4): 1-
579 11.
580 Coffer, M.M., and Hestir, E.L. (2019). Variability in trends and indicators of CO_2
581 exchange across arctic wetlands. Journal of Geophysical Research: Biogeosciences,
582 124: 1248-1264.

583 Cundy, A. and Croudace, I. (1996). Sediment accretion and recent sea-level rise in
584 the Solent, Southern England: inferences from radiometric and geochemical studies.
585 Estuarine Coastal Shelf Science, 43: 449–467.
586 Dadey, K., Janecek, T. and Klaus, A. (1992). Dry bulk density: its use and
587 determination. Proceedings Ocean Drilling Program Scientific Results 26: 551–554.
588 DeLaune, R.D. and White, J.R. (2012). Will coastal wetlands continue to sequester
589 carbon in response to an increase in global sea level?: a case study of the rapidly
590 subsiding Mississippi river deltaic plain. Climatic Change 110: 297–314.
591 Dijkema, K. (1990). Salt and Brackish Marshes Around the Baltic Sea and Adjacent
592 Parts of the North Sea: Their Vegetation and Management. Biological Conservation
593 51: 191-209.
594 Ding, Q., Schweiger, A., L'Heureux, M., Battisti, D., Po-Chedley, S., Johnson, N.,
595 Blanchard-Wrigglesworth, E., Harnos, K., Zhang, Q., Eastman, R. and Steig, E.
596 (2017). Influence of high-latitude atmospheric circulation changes on summertime
597 Arctic sea ice. Nature Climate Change 7: 289–295.
598 Doughty, C.L., Langley, J.A., Walker, W.S. Feller, I.C., Schaub, R. and Chapman, S.
599 (2016). Mangrove Range Expansion Rapidly Increases Coastal Wetland Carbon
600 Storage. Estuaries and Coasts 39: 385–396.
601 Duarte, C., Losada, I., Hendriks, I., Mazarrasa, I. and Marbà, N. (2013). The role of
602 coastal plant communities for climate change mitigation and adaptation. Nature
603 Climate Change 3: 961–968.
604 Eilertsen, H.C and Skarðhamar, J. (2006). Temperatures of north Norwegian fjords
605 and coastal waters: Variability, significance of local processes and air–sea heat
606 exchange. Estuarine, Coastal and Shelf Science, 67(3): 530-538.

607 Euskirchen, E.S., Bret-Harte, M.S., Shaver, G.R. Edgar, C.W. and Romanovsky, V.E
608 (2017). Long-Term Release of Carbon Dioxide from Arctic Tundra Ecosystems in
609 Alaska. Ecosystems 20: 960-974.
610 Eronen, M., Glückert, G., Hatakka, L., van de Plassche, O., van der Plicht, J. and
611 Rantala, P. (2001). Rates of Holocene isostatic uplift and relative sea-level lowering
612 of the Baltic in SW Finland based on studies of isolation contacts. Boreas 30: 17–30.
613 Forkel, M., Carvalhais, N., Rödenbeck, C., Keeling, R., Heimann, M., Thonicke, K.,
614 Zaehle, S. and Reichstein, M. (2016). Enhanced seasonal CO2 exchange caused by
615 amplified plant productivity in northern ecosystems. Science 12: 696-699
616 Greiner, J.T., McGlathery, K.J., Gunnell, J. and McKee, B.A. (2013). Seagrass
617 Restoration Enhances “Blue Carbon” Sequestration in Coastal Waters. PLoS
618 ONE 8(8): e72469
619 Harvey, J.W., Chambers, R.M. and Hoelscher, J.R. (1995). Preferential flow and
620 segregation of porewater solutes in wetland sediment. Estuaries 18(4): 568–578.
621 Henningsson, S. and Alerstam, T. (2005). Barriers and distances as determinants for
622 the evolution of bird migration links: the arctic shorebird system. Proceedings of the
623 Royal Society B 2722251–2258
624 Howard, J., Hoyt, S., Isensee, K., Telszewski, M., Pidgeon, E. (eds)(2014) Coastal
625 Blue Carbon: Methods for Assessing Carbon Stocks and Emissions Factors inb
626 Mangroves, Tidal salt Marshes, and Seagrasses. Conservation International,
627 Intergovernmental Oceanographic Commission of UNESCO, International Union for
628 Conservation of Nature. Arlington, Virginia, USA.
629 IPCC (2013) Climate change 2013: Summary for Policymakers. Cambridge
630 University Press, UK.

631 Ju, J. and Masek, J. (2016). The vegetation greenness trend in Canada and US
632 Alaska from 1984–2012 Landsat data. Remote Sensing of Environment 176: 1-16.
633 Kirwan, M. and Mudd, S. (2012). Response of salt-marsh carbon accumulation to
634 climate change. Nature 489: 550-554.
635 Lal, R. (2004). Soil carbon sequestration to mitigate climate change. Geoderma 123:
636 1-22.
637 Levell, B.K. (1980). A late Precambrian tidal shelf deposit, the Lower Sandfjord
638 Formation, Finnmark, North Norway. Sedimentology, 27: 539-557.
639 Li, Y., Wang, L., Zhang, W., Zhang, S., Wang, H., Fu, X. and Le, Y. (2010) Variability
640 of soil carbon sequestration capability and microbial activity of different types of salt
641 marsh soils at Chongming Dongtan. Ecological Engineering 36: 1754-1760.
642 Lima, M., Ward, R., and Joyce, C. (2020). Environmental drivers of carbon stocks in
643 temperate seagrass meadows. Hydrobiologia 847: 1773–1792
644 Lovelock, C.E. and Duarte, C.M. (2019). Dimensions of Blue Carbon and emerging
645 perspectives. Biological Letters 15: 20180781.
646 Mafi-Gholami, D., Zenner, E., Jaafari, A., & Ward, R. (2018). Modeling multi-decadal
647 mangrove leaf area index in response to drought along the semi-arid southern
648 coasts of Iran. Science of the Total Environment 656: 1326-1336
649 Martini, P., Morrison, G., Abraham, K., Sergienko, L., Jefferies, R. (2019). Northern
650 Polar Coastal Wetlands: Development, Structure, and Land Use. In: Perillo, G.,
651 Wolanski, E., Cahoon, D. and Hopkinson, C. Coastal Wetlands, Elsevier,
652 Netherlands.
653 MET Norway (2019). Data from The Norwegian Meteorological Institute.
654 www.eKlima.no. Norway.

655 NGU (2017). Norwegian Geological Survey Web Map Server. Norwegian Geological
656 Survey, Norway.
657 Osland, M.J., Enwright, N.M., Day, R.H., Gabler, C.A., Stagg, C.L. and Grace, J.B.
658 (2016). Beyond just sea-level rise: considering macroclimatic drivers within coastal
659 wetland vulnerability assessments to climate change. Global Change Biology 22: 1-
660 11.
661 Park, T., Ganguly, S., Tømmervik, H., Eugénie, E., Høgda, K., Karlsen, S., Brovkin,
662 V., Nemani, R. and Myneni, R. (2016). Changes in growing season duration and
663 productivity of northern vegetation inferred from long-term remote sensing data.
664 Environmental Research Letters 11(8): 084001.
665 Pendleton, L., Donato, D.C., Murray, B.C., Crooks, S., Jenkins, W.A., Sifleet. S.,
666 Craft, C., Fourqurean, J., Kauffman, J., Marba, N., Megonigal, P., Pidgeon, E., Herr,
667 D., Gordon, D. and Balder, A. (2012). Estimating Global ‘‘Blue Carbon’’ Emissions
668 from Conversion and Degradation of Vegetated Coastal Ecosystems. PLoS ONE
669 7(9): e43542.
670 Plater, A.J. and Appleby, P.G. (2004). Tidal sedimentation in the Tees estuary during
671 the 20th century: radionuclide and magnetic evidence of pollution and sedimentary
672 response. Estuarine Coastal Shelf Science, 60: 179–192.
673 Povinec, P.P., Bailly du Bois, P., Kershaw, P.J., Neis, H. and Scotto, P. (2003).
674 Temporal and spatial trends in the distribution of 137Cs in surface waters of
675 Northern European Seas — a record of 40 years of investigations. Deep-Sea
676 Research 50: 2785–280.
677 Powlson, D., Whitmore, A. and Goulding, W. (2011). Soil carbon sequestration to
678 mitigate climate change: a critical re-examination to identify the true and the false.
679 European Journal of Soil Science 62: 42-55.

680 Rahmstorf, S. (2010). A new view on sea level rise. Nature Reports Climate Change
681 4: 44-45.
682 Ratas, U. and Nilson, E. (1997) Small Islands of Estonia. Institute of Ecology,
683 Estonia.
684 Ritchie, J.C., McHenry, J.R., (1990). Application of radioactive fallout caesium-137
685 for measuring soil erosion and sediment accumulation rates and patterns: a review.
686 Journal Environmental Quality, 19: 215–233.
687 Roberts, D., Olesen, O. and Karpuz, M.R. (1997). Seismo- and neotectonics in
688 Finnmark, Kola Peninsula and the southern Barents Sea. Part 1: Geological and
689 neotectonic framework. Tectonophysics, 270: 1-13.
690 Rosen, K., Vinichuk, M. and Johanson, K. (2009). 137Cs in a raised bog in central
691 Sweden. Journal of Environmental Radioactivity 100(7): 534–539
692 Saintilan, N., Rogers, K., Kelleway, J.J., Ens, E. and Sloane, D.R. (2019). Climate
693 Change Impacts on the Coastal Wetlands of Australia. Wetlands 39: 1145–1154.
694 Smoak, J., Breithaupt, J., Smith, T. and Sanders, C. (2013) Sediment accretion and
695 organic carbon burial relative to sea-level rise and storm events in two mangrove
696 forests in Everglades National Park. Catena 104: 58-66.
697 Symon, C., Arris, L. and Heal, B. (2005). Arctic Climate Impact Assessment.
698 Cambridge University Press, UK.
699 Teasdale, P., Collins, P., Firth, C. and Cundy, A. (2011). Recent estuarine
700 sedimentation rates from shallow inter-tidal environments in western Scotland:
701 implications for future sea-level trends and coastal wetland development. Quaternary
702 Science Reviews, 30: 109–129.

703 Thompson, J., Dyer, F.M. and Croudace, I.W., (2001). Records of radionuclide
704 deposition in two U.K. salt marshes in the United Kingdom with contrasting redox
705 and accumulation conditions. Geochimica Cosmochimica Acta, 66: 1011–1023.
706 Trask, P.D. (1932). Origin and Environment of Source Sediments of Petroleum,
707 Houston. Gulf Publication Company, Houston, USA.
708 Veettil, B., Ward, R., Lima, M., Stankovic, M. and Quang, N. (in press). Opportunities
709 for seagrass research derived from remote sensing: a review of current methods.
710 Ecological Indicators.
711 Walker, D., Epstein, H., Raynolds, M., Kuss, P., Kopecky, M., Frost, G., Daniëls, F.,
712 Leibman, M., Moskalenko, N., Matyshak, G., Khitun, O., Khomutov, A., Forbes, A.,
713 Bhatt, U., Kade, A., Vonlanthen, C. and Tich, L. (2012). Environment, vegetation and
714 greenness (NDVI) along the North America and Eurasia Arctic transects.
715 Environment Research Letters, 7: 015504
716 Ward, R. (2020). Sedimentary response of Arctic coastal wetlands to sea level rise.
717 Geomorphology in press.
718 Ward, R., Friess, D., Day, R., and Mackenzie, R. (2016c). Impacts of Climate
719 Change on Global Mangrove Ecosystems: A Regional Comparison. Ecosystem
720 Health and Sustainability 2(4): 1-25
721 Ward, R., Burnside, N., Joyce, C. and Sepp, K. (2016a). Importance of micro-
722 topography in determining plant community distribution in Baltic coastal wetlands.
723 Journal of Coastal Research 32(5): 1062-1070
724 Ward, R., Burnside, N., Joyce, C., Sepp, K. and Teasdale, P. A. (2014) Recent rates
725 of sedimentation on irregularly flooded Boreal Baltic coastal wetlands: responses to
726 recent changes in sea level Geomorphology 217: 61-72

727 Ward, R., Burnside, N., Joyce, C., Sepp, K. and Teasdale, P. A. (2016b). Improved
728 modelling of the impacts of sea level rise on coastal wetland plant communities.
729 Hydrobiologia Wetlands Biodiversity & Processes: 1-14.
730 Wassmann, P., Svendsen, H., Keck, A. and Reigstad, M. 1996. Selected aspects of
731 the physical oceanography and particle fluxes in fjords of northern Norway. Journal
732 of Marine Systems, 8: 1-2: 53-71.
733 Wise, S.M. (1980). Caesium-137 and lead-210: a review of the techniques and some
734 applications in geomorphology. In: Cullingford, R.A., Davidson, D.A., Lewin, J.
735 (Eds.),
736 Timescales in Geomorphology. John Wiley and Sons Ltd., pp. 109–127.
737 Yu, Q., Epstein, H., Engstrom, R. and Walker, D. (2017), Circumpolar arctic tundra
738 biomass and productivity dynamics in response to projected climate change and
739 herbivory. Global Change Biology 23: 3895-3907.

Table

Click here to download Table: Table 1.docx

Site name	Latitude (DD)	Longitude (DD)	Average annual temperature (°C)	Average annual precipitation (mm)	Length of the growing season (days)
Alta	69.9783	23.4315	2.5	431	118
Stabbursnes	70.1942	24.9275	1.8	403	110
Birtvarre	69.4959	20.8204	3.6	1006	130
Storfjord	69.2713	19.9266	2.9	401	125
Storslett	69.7819	20.9953	2.5	782	119

Table

Click here to download Table: Table 2.docx

Site	^{210}Pb EAD 1963	^{210}Pb EAD 1986
Alta LM	1957	1983
Alta HM	1924	1946
Stabbursnes LM	1957	1984
Stabbursnes HM	1955	1991
Birtvarre LM	1966	1998
Birtvarre HM	1951	1976
Storfjord LM	1919	1973
Storfjord HM	BMD	1974
Storslett LM	BMD	1941
Storslett HM	1934	1987

Table

Click here to download Table: Table 3.docx

Sites	Average sequestration rates (gC m^2 $year^{-1}$)	
	1963	1986
Alta low marsh	17	13
Alta high marsh	46	22
Stabbursnes low marsh	450	593
Stabbursnes high marsh	326	340
Birtvarre low marsh	56	63
Birtvarre high marsh	973	1277
Storfjord low marsh	1337	1569
Storfjord high marsh	540	372
Storslett low marsh	374	389
Storslett high marsh	378	856

Table

Click here to download Table: Table 4.docx

Sites	Average sequestration rates (gC m^2 $year^{-1}$)		No. of years analysed (LM, HM)
	Low marsh	High marsh	
Alta	19	22	70, 133
Stabbursnes	260	321	100, 92
Birtvarre	49	603	100, 102
Storfjord	390	340	95, 77
Storslett	368	159	116, 144

Table

Click here to download Table: Table 5.docx

	MgC ha^{-1}	
Site	Low marsh	High marsh
Alta	3.74	3.67
Birtvarre	6.29	5.15
Storfjord	10.53	3.96
Storslett	6.31	13.79
Stabbursnes	5.68	3.82

Table

Click here to download Table: Table 6.docx

Environmental variable	Sequestration rate	Sorting coefficient	d50	Growing season	Precipitation
Sequestration rate					
Sorting coefficient	0.092				
d50	-0.333	-0.076			
Growing season	0.815***	-0.050	-0.229		
Precipitation	0.455	-0.155	-0.651*	0.370	
Sea level rise	-0.344	-0.220	-0.320	0.053	0.083

Figure

Click here to download high resolution image

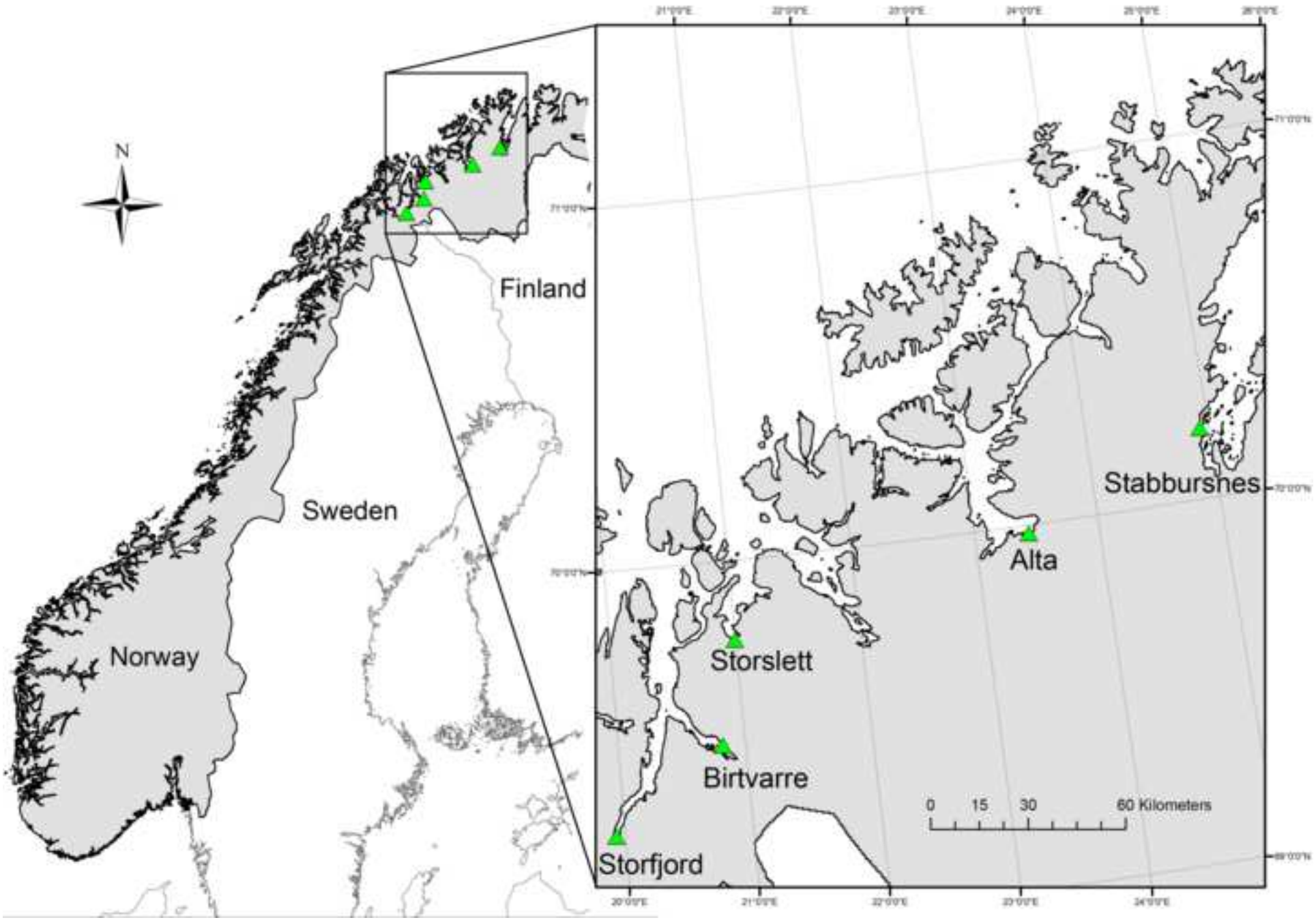

Figure

Click here to download high resolution image

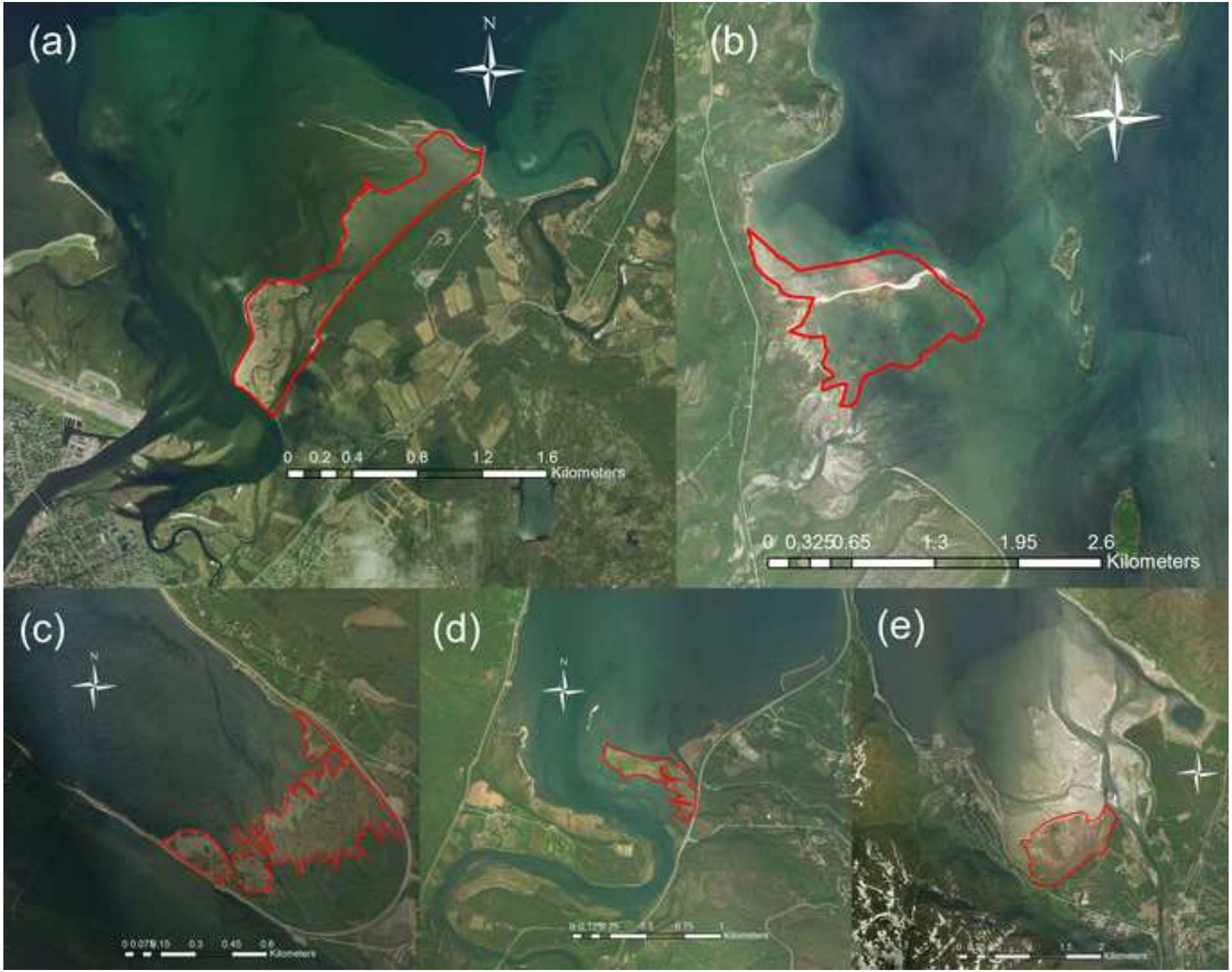

Figure

Click here to download high resolution image

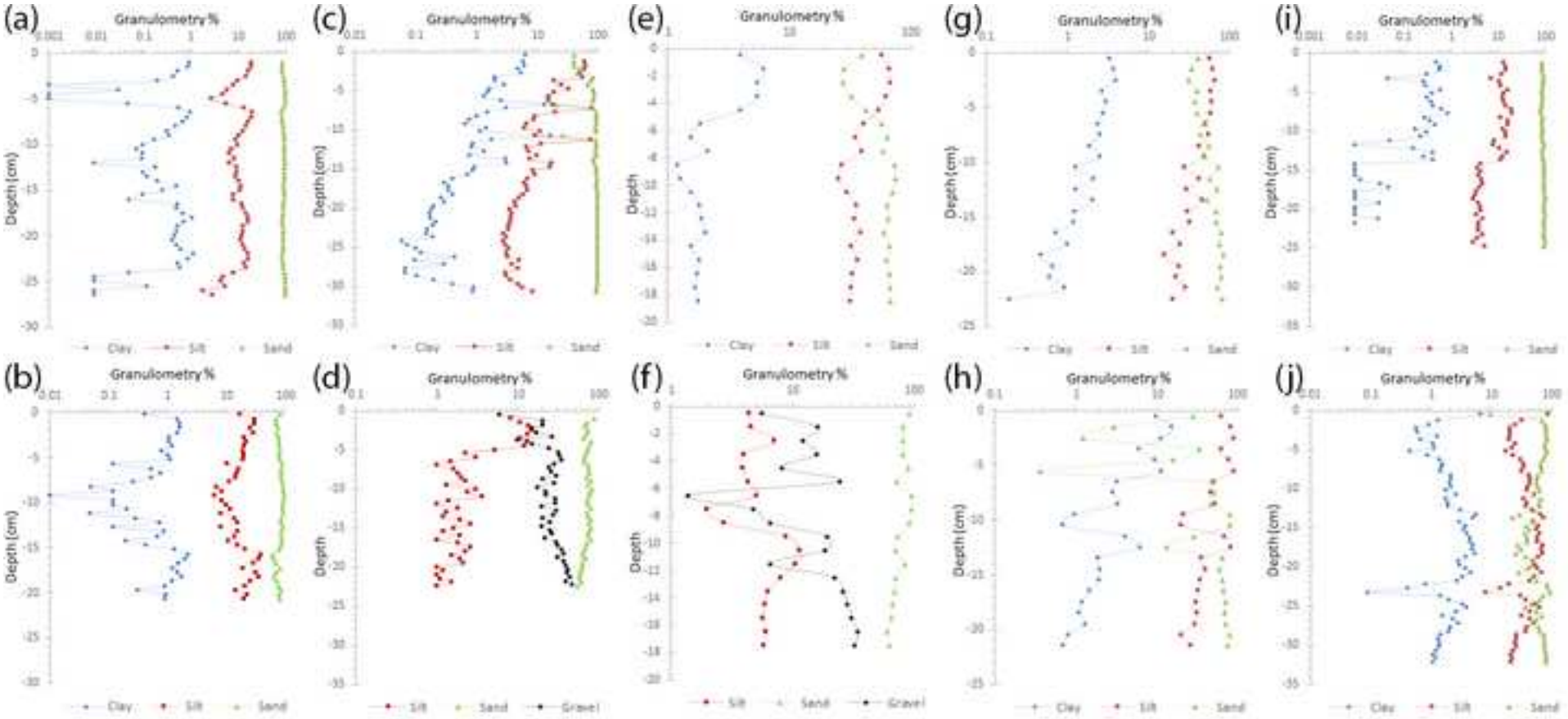

Figure

Click here to download high resolution image

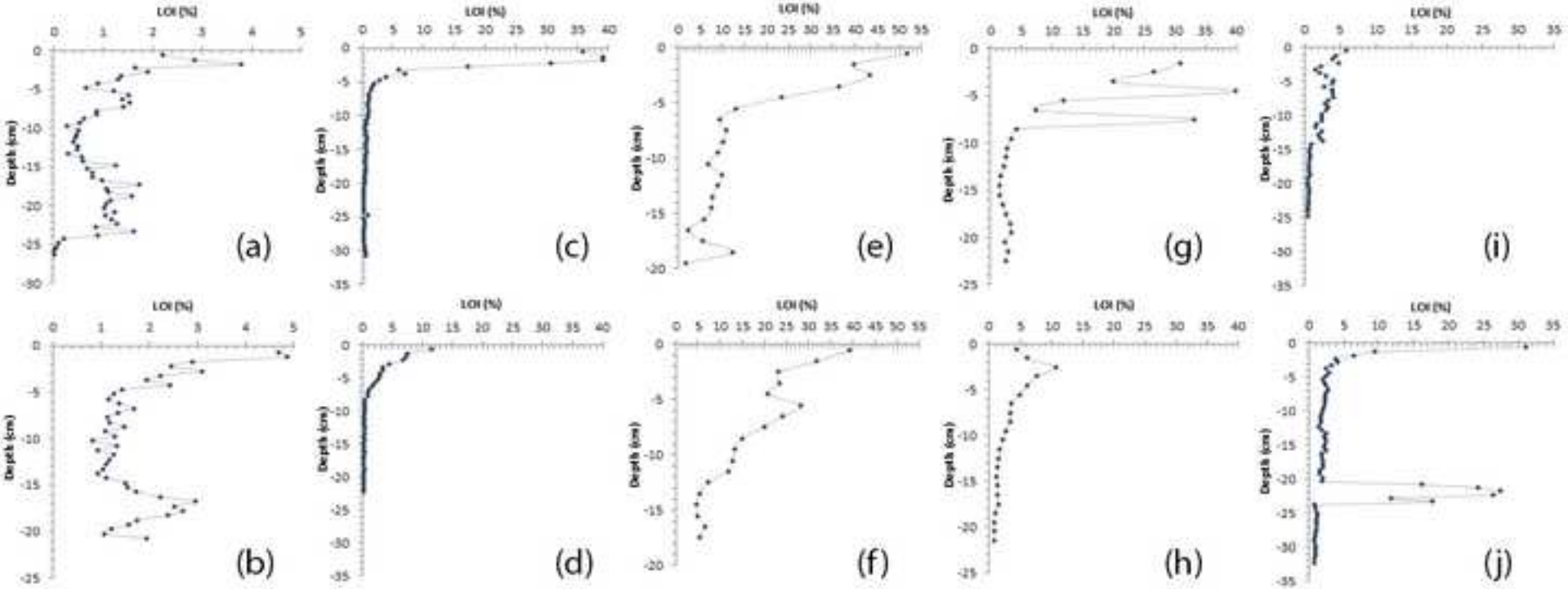

Figure

Click here to download high resolution image

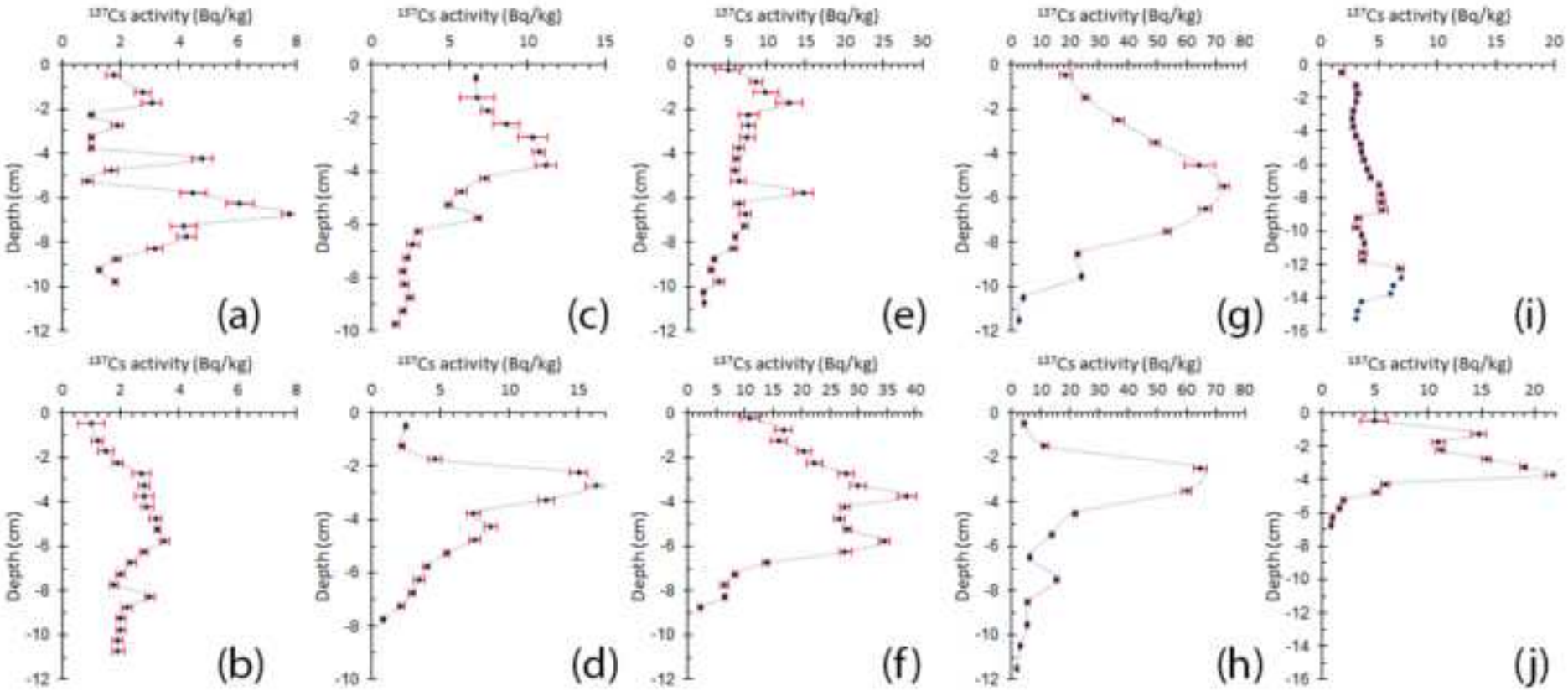

Figure

Click here to download high resolution image

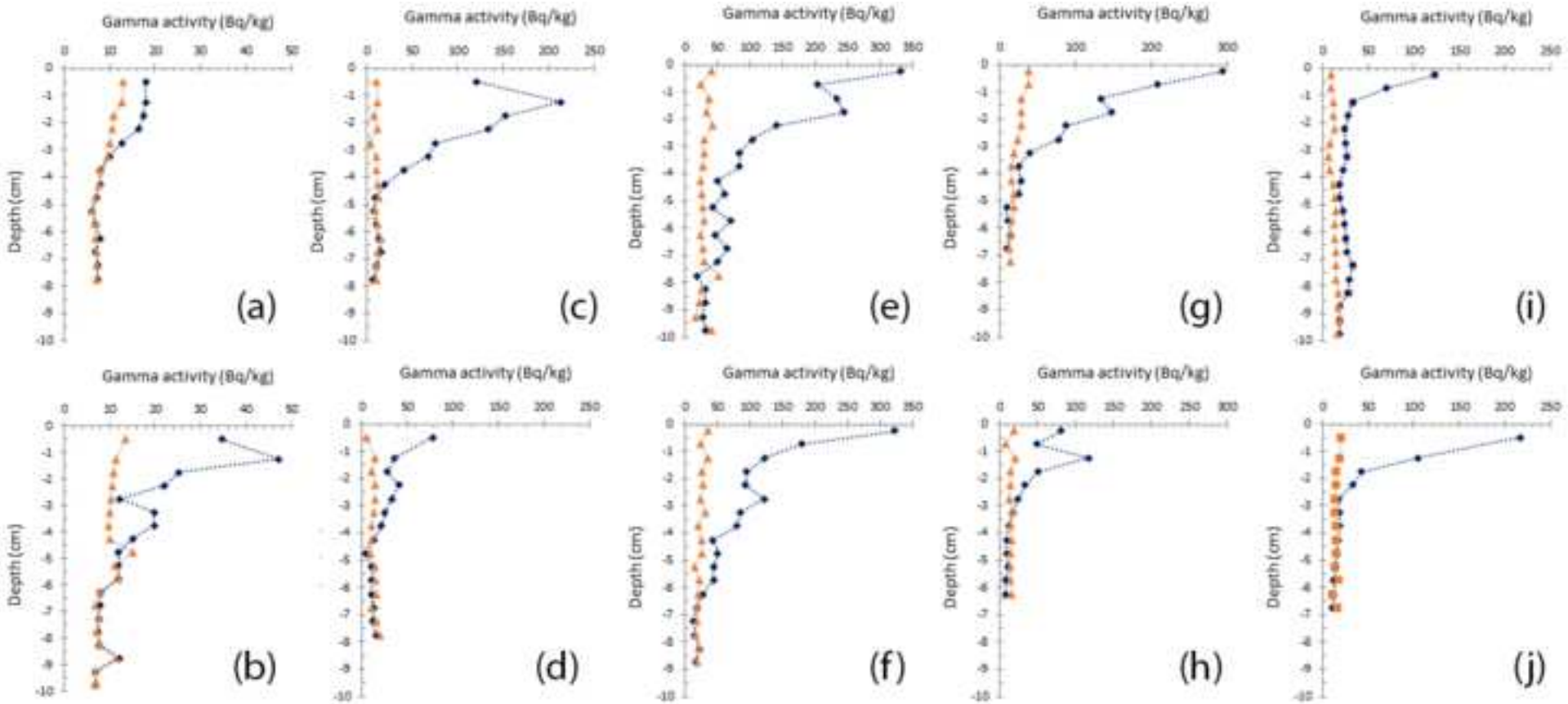

Figure

Click here to download high resolution image

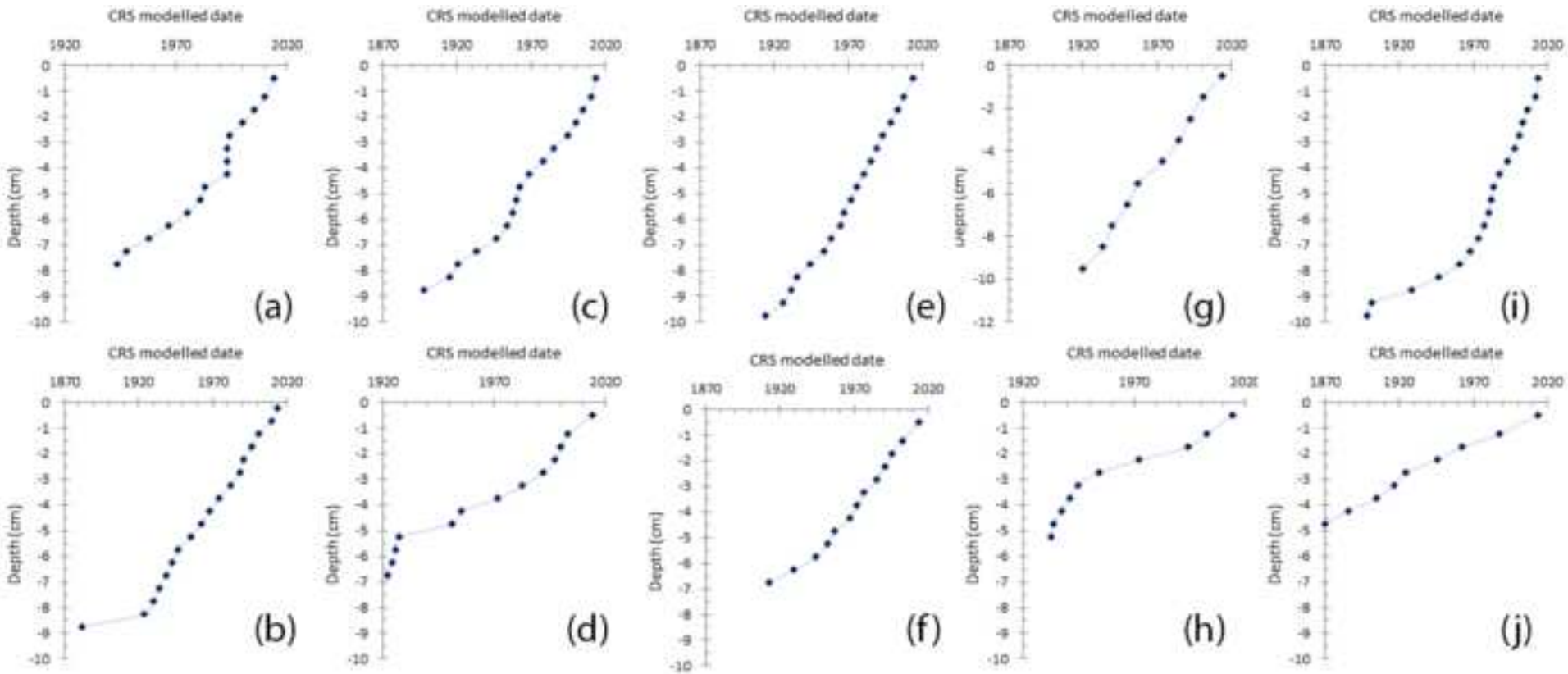

Figure

Click here to download high resolution image